
THE COOPERATION-DEFECTION EVOLUTION ON SOCIAL NETWORKS

A PREPRINT

 **Bijan Sarkar***

Department of Mathematics
Neotia Institute of Technology, Management and Science
Diamond Harbour Road, 24 Parganas (South)
West Bengal-743368, India
bijan0317@yahoo.com

June 4, 2022

ABSTRACT

Without contributing, defectors take more benefit from social resources than cooperators which is the reflection of a specific character of individuals. However, the natural physical mechanisms of our society promote cooperation. Thus, in the long run, the evolution about genetic variation is something more than the social evolution about fitness. The loci of evolutionary paths of the cooperation and the defection are correlated, but not full complement of each other. Yet, the only single specific mechanism which is operated by some rules explains the enhancement of cooperation where the independent analysis of defect evolutionary mechanism is ignored. Moreover, the execution of a particular evolutionary rule through algorithm method over the long time experiences highly sensitive influence of the model parameters. Theoretically, biodiversity of two types relatively persists rarely. Here I describe the evolutionary outcome in the demographic fluctuation. Using both analytical procedure and algorithm method the article concludes that the intratype fitness of individual species is the key factor for not only surviving, but thriving. In consideration of the random drift, the experimental outcomes show that dominant enhancement of cooperation over defection is qualitatively independent of environmental scenario. Collectively, the set of the rules becomes an evolutionary principle to cooperation enhancement.

Keywords evolutionary game theory · analytical procedure · algorithm method · cooperation enhancement · defection hindrance

1 Introduction

The demographic fluctuation is not the consequence of a particular account of evolutionary structure[1, 2, 3]. It is partly an effect of the random fluctuation in the result of the combination of various genetic, ecological and sociological factors such as selection, reproduction, mutation, migration, etc. The factors collectively play a role in the struggle for existence [4]. Thus, a random drift on the evolutionary structure would be needed to explain the stochastic effect of demographic fluctuation. As the clarification of this effect can be based on some logical structure, it obviously has deterministic interpretation. Here, we explore the random fluctuation features by adopting the concept of individuals' attachment and leaving tendency to a social network. It has generally found that any kind of regularity break in the social structure pattern in the sense of either geometry or individual reputation and punishment help to cooperation enhancement. However, it is not true in all circumstances at all [5, 6].

We already know that the stochastic effects become less important for large population size [7]. In the continuation, it is also true that the existence of non Darwinian dynamics can only expect under the random scenarios. Thus, how the local evolution of each of the hub populations affecting on global evolutionary dynamics is one of the important

*E-mail: bijan0317@gmail.com

subjects of evolutionary research work, where the term hub best suits for small, simple neighbourhood area network environment of a focal node.

We consider a social network by a simple graph structure of \mathcal{N} vertices. Every vertex is occupied by a cooperator individual (C), occupied by a defector individual (D) or vacant – the place which could be occupied by any one of the two types (or species) of individuals. Two individuals can interact only if they are connected by an edge of the graph. We confine ourselves in on the random regular graphs, however, implementing the model concept for the heterogeneous complex networks is straightforward. The evolution is interpreted here by the genetic reproduction, and the model formalism is well fitted for the both asexual and sexual contexts. Besides the birth-death update event, the synchronous formulation accounts the random drift effect while the internal migration is overlooked.

In the social pool, the evolutionary process advances through the function of the fitness values of the individuals, where the fitness measures by the combination of the fertility effect and the viability effect on gene C and gene D [8, 9]. The effective fitness generally is studied at the reproduction level of an individual [10]. The fitness means the effective fitness here. We consider the standard payoff matrix of a two-player version of the interaction for the representing the fitness values, π_{**} , of the row individual. According to the base matrix of such interaction, cooperators pay a cost to provide a benefit while defectors neither pay cost nor contribute benefit.

Under the evolutionary game theory framework the birth-death evolution can robustly define the evolutionary dynamics of pure Darwinian selection [11, 12, 13]. To explain the emergence of cooperation it is mainly emphasised on the configurational arrangement of individuals in their residential areas where the total population size is always fixed over time. Assuming so, the derived rules of the analytically tractable model, based on the formalisms like Hamilton's rule [14, 15, 16] as well as the static game property like Evolutionarily Stable Strategy [17], are able to figure out the ubiquitous character of cooperation. However, every rule has its own limitation, and they fail over long ranges of biological parameters [18]. Thereby, instead of emergence principle the emergence theory has been compelled to rely on some specific rules of limiting evolutionary cases, up until now.

Based on the experimental outcome obtained by using both analytical procedure and algorithm method where the procedure and the method are derived through a trick of the putting mathematical tractability before empirical evidence in this article we infer that the intratype fitness of individual species is the key factor for cooperation enhancement and defection hindrance. A set of five self-explanatory observables clarifies the whole experimental outcome. In following the slightly non-conventional way our aim is to demonstrate that in the distinct mechanisms of cooperation and defection, natural cooperation is a principle of evolution.

2 The model

The outcome of the evolution is the result of the combined effects of the two completely independent events: one is the birth-death event, and the other is the random drift event [19]. In the underlying mechanism of birth-death, the expectation value of transition individuals over each of the population hubs has been calculated with respect of an evolution probability, where the product of the segregation probability and the reproduction-demise probability determines the probability mass function, i.e. the evolution probability. And, finally the expectation of all calculated expectation values of transition individuals over all possible hub sizes measures the evolution rate change per unit time span due to the birth-death event. The other independent event, the random drift, completely is captured within the probability space, Ω , that being defined by two parameter variables: p is the probability of attachment of a new individual to the network and q is the probability of leaving of an individual from the network (Fig. 1). The fractional concentration variables, x and y corresponding to cooperators and defectors respectively, represent the explicit form of the evolutionary dynamics as:

$$\begin{aligned}\frac{\partial x}{\partial t} &= a_3\left(\frac{x}{x+y}\right)^3 + a_2\left(\frac{x}{x+y}\right)^2 + a_1\left(\frac{x}{x+y}\right) + \sigma_x \bar{\nabla}^2 x, \\ \frac{\partial y}{\partial t} &= b_3\left(\frac{y}{x+y}\right)^3 + b_2\left(\frac{y}{x+y}\right)^2 + b_1\left(\frac{y}{x+y}\right) + \sigma_y \bar{\nabla}^2 y,\end{aligned}$$

where a_* s and b_* s are the mathematical functions of fitness, graph degree, and σ_* s are the coefficients of the random drift. The term concentration means the spatial density here.

The algorithm version of the same dynamical system is examined not only for optimizing our pursuance but also for determining the initial direction of evolutionary dynamics because the direction determination in the randomness pattern by utilising the Monte Carlo simulation procedure [20] is essential for the analytical version. The components

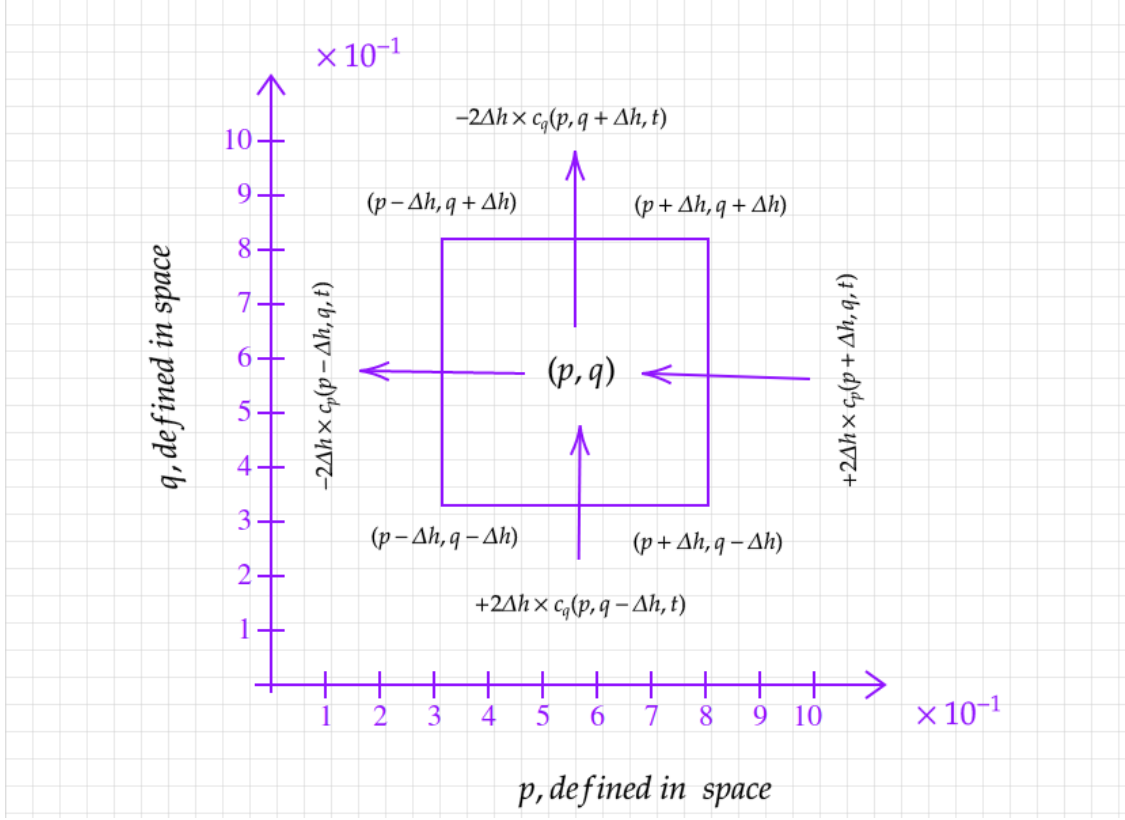


Figure 1: An accumulation of individuals through the random drift in a small area, $(2\Delta h)^2$, on the probability space Ω . The Ω is embedded into the geometrical space of the considering network. The arbitrary coordinate (p, q) assigns the centre position, having the concentration $c(p, q, t)$. The signs, positive and negative point out the relative possibility of the attachment and the leaving of the individuals, respectively. The net effect of a random drift on average concentration of an individual type is a simple sum of the two resultant flux terms of each of the directions where the direction of arrows indicates the directions of the impact of the random drift. This is the schematic presentation of the physical interpretation of the term, $\nabla^2 c = (\frac{\partial^2}{\partial p^2} - \frac{\partial^2}{\partial q^2})c$. The randomness of the term intuitively understands through the sign convention. The probability to occur each sign at a particular point may assume to be equal to 0.5 and the factor 0.5 is part of the σ_* .

of the Moran process determine the reproduction-demise probabilities; and this determination sets the birth-death rules in the algorithm version. The birth takes place if

$$\text{random}() < \frac{\text{fitness of an individual}}{\text{maximum fitness of each individual}},$$

where the death of an individual occurs if

$$\text{random}() < \frac{\text{number of same type neighbour individuals}}{\text{total number of neighbour individuals}}.$$

The independent rules are valid until the presence of at least one same type individual of the focal individual. The standard library function, $\text{random}()$, generates a random number at each of the iterative steps. Instead of the segregation probability – defined by the binomial distribution configuration – the algorithm method uses the manual approach to measure the segregation tendency. Both the probabilities act at the individual level, not at the gene level. In the other event, the random drift rule of an attachment individual set to: $\text{random}() < p \cdot \sigma_*$, while the random drift rule of a leaving individual set to: $\text{random}() < q \cdot \sigma_*$, where determination of the preferential selection type individual for the leaving or the attaching is needed which is described by the majority selection rule.

2.1 The analytical version of the evolutionary dynamics

The overall system is captured on the belief of the evolution of individual character not depending on the specific architecture of the network/spatial structure; instead, it is dependent on the average number of neighbours of the focal individual. The system environment comprises of cooperators and defectors, having the normal carrying capacity \mathcal{N} . Now, we take $P(i, j, t)$ is the probability that there are i cooperator individuals and j defector individuals at the time t , and denote the increasing and decreasing transition rates of the population from one state to its neighbouring state as T_*^+ and T_*^- respectively, with appropriate subscripts – the explanation is that in per unit time, through the rate T_{i-1}^+ the state $i-1$ switches to the next neighbouring state i while through the rate T_i^- the state i switches to the next neighbouring state $i-1$. In the time duration Δt , replacing the simple rate laws by probability laws we have

$$\begin{aligned} P(i, j, t + \Delta t) - P(i, j, t) &= T_{i-1}^+ P(i-1, j, t) + T_{j-1}^+ P(i, j-1, t) + T_{i+1}^- P(i+1, j, t) \\ &\quad + T_{j+1}^- P(i, j+1, t) - (T_i^+ + T_j^+ + T_i^- + T_j^-) P(i, j, t). \end{aligned} \quad (1)$$

The system dynamics is generally described by the above master equation [21]. In the present frontier, we shall show that based on this probability law, we shall be able to derive the two separate time dependent loci of evolutionary dynamics, one for cooperator group and the other for defector group following the special mathematical tractability, so that the system dynamics can be portrayed explicitly.

Keeping in mind the driving fact of random drift like diffusion [22] directed towards the lower concentration state, in order to convert from the discrete to the continuous state doing slight modification of some appropriate terms in the master equation, the locus of the evolutionary dynamics of cooperation in the presence of the i -number of cooperator individuals, on the continuous state, can be extracted as

$$\begin{aligned} iP(i, j, t + \Delta t) - iP(i, j, t) &= \{0 \cdot T_{i-1}^+ P(i-1, j, t) + 0 \cdot T_{j-1}^+ P(i, j-1, t) \\ &\quad + iT_{i+1}^- P(i+1, j, t) + 0 \cdot T_{j+1}^- P(i, j+1, t) \\ &\quad - [-iT_i^+ + 0 \cdot T_j^+ + 2iT_i^- + 0 \cdot T_j^-] P(i, j, t)\} \Delta t \\ \implies \sum_{i=0}^{\mathcal{N}} \sum_{j=0}^{\mathcal{N}-i} [iP(i, j, t + \Delta t) - iP(i, j, t)] &= \sum_{i=0}^{\mathcal{N}} \sum_{j=0}^{\mathcal{N}-i} \{iT_i^+ P(i, j, t) - iT_i^- P(i, j, t) \\ &\quad + \underbrace{iT_{i+1}^- P(i+1, j, t) - iT_i^- P(i, j, t)}_{\text{random drift effect}}\} \Delta t. \end{aligned} \quad (2)$$

Similarly, using the same master equation the locus of the evolutionary dynamics of defection in the presence of the j -number of defector individuals, on the continuous state, can be extracted as

$$\begin{aligned} jP(i, j, t + \Delta t) - jP(i, j, t) &= \{0 \cdot T_{i-1}^+ P(i-1, j, t) + 0 \cdot T_{j-1}^+ P(i, j-1, t) \\ &\quad + 0 \cdot T_{i+1}^- P(i+1, j, t) + jT_{j+1}^- P(i, j+1, t) \\ &\quad - [0 \cdot T_i^+ - jT_j^+ + 0 \cdot T_i^- + 2jT_j^-] P(i, j, t)\} \Delta t \\ \implies \sum_{j=0}^{\mathcal{N}} \sum_{i=0}^{\mathcal{N}-j} [jP(i, j, t + \Delta t) - jP(i, j, t)] &= \sum_{j=0}^{\mathcal{N}} \sum_{i=0}^{\mathcal{N}-j} \{jT_j^+ P(i, j, t) - jT_j^- P(i, j, t) \\ &\quad + \underbrace{jT_{j+1}^- P(i, j+1, t) - jT_j^- P(i, j, t)}_{\text{random drift effect}}\} \Delta t. \end{aligned} \quad (3)$$

Next, we have to calculate each term of each equation with following the specific mathematical tractability in view of the simple natural rules.

- The segregation probability is expanded in a Taylor series at t upto the second order in Δt and the fact $x' = \sum_{i=0}^{\mathcal{N}} \sum_{j=0}^{\mathcal{N}-i} iP(i, j, t) = \sum_{i=0}^{\mathcal{N}} iP_i(i, t)$ yields that

$$\begin{aligned}
\sum_{i=0}^{\mathcal{N}} \sum_{j=0}^{\mathcal{N}-i} [iP(i, j, t + \Delta t) - iP(i, j, t)] &= \sum_{i=0}^{\mathcal{N}} \left[\frac{\partial}{\partial t} iP_i(i, t) \right] \Delta t + \mathcal{O}(\Delta t)^2 \\
&= \frac{\partial x'}{\partial t} \Delta t + \mathcal{O}(\Delta t)^2.
\end{aligned} \tag{4}$$

Similarly, the segregation probability is expanded in a Taylor series at t upto the second order in Δt and the fact $y' = \sum_{j=0}^{\mathcal{N}} \sum_{i=0}^{\mathcal{N}-j} jP(i, j, t) = \sum_{j=0}^{\mathcal{N}} jP_j(j, t)$ yields that

$$\begin{aligned}
\sum_{j=0}^{\mathcal{N}} \sum_{i=0}^{\mathcal{N}-j} [jP(i, j, t + \Delta t) - jP(i, j, t)] &= \sum_{j=0}^{\mathcal{N}} \left[\frac{\partial}{\partial t} jP_j(j, t) \right] \Delta t + \mathcal{O}(\Delta t)^2 \\
&= \frac{\partial y'}{\partial t} \Delta t + \mathcal{O}(\Delta t)^2.
\end{aligned} \tag{5}$$

- In this step, to measure the equality, we have to define the segregation probability which is represented by P , and the reproduction-demise probability which is represented by T . As according to the order of genetic reproduction action, the segregation of genes takes place before the natural selection, thus here the segregation probability plays a role of fertility selection which is nothing but the effect of social arrangement of two types of individuals while the natural selection role is played by the reproduction-demise probability. However, in the main master equation the order of the action of two probability terms might be different, first we could count the reproduction-demise probability then the next would be to count the segregation probability, or vice-versa. This is obvious because in the component wise representation of master equations a specific number of individuals is assumed at particular times of t where we confine ourselves in the three consecutive cooperator levels: $(i - 1)^{th}$ level, i^{th} level and $(i + 1)^{th}$ level as well as in the similar levels for defectors. In the present treatise we follow the natural order, first the fertility selection and then after the natural selection at the same social structure, and due to following this order, we are able not only to carry out the local hub calculation but can also extend the calculation to the whole network structure. One can agree based on such pattern of binomial distribution of two different characters of individuals that, the spatial or configurational arrangement or fertility effect is to be perfectly defined by Wright-Fisher transition probability in terms of the expected numbers of cooperators and defectors at particular times t because the Wright-Fisher transition probability is some extend a more general version of the reproduction rule than the majority selection updating rule, while the reproduction-demise probability is proper fit to the selection component of Moran transition probability. To extend the local hub calculation, we consider the system environment is a connected graph with \mathcal{N} vertices and degree distribution $p(k)$. Therefore, with a note that $z = \sum k p(k)$ and defining the normalised fitness constant Γ_{max} in the averagely sense of optimum fitness of an individual, such that $\Gamma_{max} \geq average\{\pi_{CC}, \pi_{CD}, \pi_{DC}, \pi_{DD}\}$, in the limit of $\Delta t \rightarrow 0$ we have ²

$$\begin{aligned}
\lim_{\Delta t \rightarrow 0} \frac{1}{\Delta t} \sum_{i=0}^{\mathcal{N}} \sum_{j=0}^{\mathcal{N}-i} [iT_i^+ P(i, j, t)] \Delta t &= \sum_{i=0}^{\mathcal{N}} iT_i^+ P_i(i, t) \\
&= \sum_{k=1}^{\mathcal{N}-1} p(k) \sum_{i=0}^k iT_i^+ P_i(i, t) \\
&= \sum_{k=1}^{\mathcal{N}-1} p(k) \sum_{i=0}^k i \frac{k!}{i!(k-i)!} \left(\frac{x'}{x'+y'}\right)^i \left(\frac{y'}{x'+y'}\right)^{(k-i)} \\
&\quad \times \frac{i}{z\Gamma_{max}} \left(\frac{x'}{x'+y'}\pi_{CC} + \frac{y'}{x'+y'}\pi_{CD}\right) \\
&= \left\{ \frac{1}{\Gamma_{max}} \left(\frac{x'}{x'+y'}\right) + \left(\frac{\sigma^2 + z^2 - z}{z\Gamma_{max}}\right) \left(\frac{x'}{x'+y'}\right)^2 \right\} \\
&\quad \times [\pi_{CD} + (\pi_{CC} - \pi_{CD}) \left(\frac{x'}{x'+y'}\right)].
\end{aligned} \tag{6}$$

Similarly, in the limit of $\Delta t \rightarrow 0$, we have

²Note: Expectation of square of a random variable is equal to variance plus square of the expectation of the random variable.

$$\begin{aligned}
\lim_{\Delta t \rightarrow 0} \frac{1}{\Delta t} \sum_{j=0}^{\mathcal{N}} \sum_{i=0}^{\mathcal{N}-j} [jT_j^+ P(i, j, t)] \Delta t &= \sum_{j=0}^{\mathcal{N}} jT_j^+ P_j(j, t) \\
&= \left\{ \frac{1}{\Gamma_{max}} \left(\frac{y'}{x' + y'} \right) + \left(\frac{\sigma^2 + z^2 - z}{z\Gamma_{max}} \right) \left(\frac{y'}{x' + y'} \right)^2 \right\} \\
&\quad \times [\pi_{DC} + (\pi_{DD} - \pi_{DC}) \left(\frac{y'}{x' + y'} \right)]. \tag{7}
\end{aligned}$$

- In this mathematical part, the reproduction-demise probability is proper fit by the demise component of Moran transition probability where the local hub calculation is extended by the following manner:

$$\begin{aligned}
\lim_{\Delta t \rightarrow 0} \frac{1}{\Delta t} \sum_{i=0}^{\mathcal{N}} \sum_{j=0}^{\mathcal{N}-i} [iT_i^- P(i, j, t)] \Delta t &= \sum_{i=0}^{\mathcal{N}} iT_i^- P_i(i, t) \\
&= \sum_{k=1}^{\mathcal{N}-1} p(k) \sum_{i=0}^k iT_i^- P_i(i, t) \\
&= \sum_{k=1}^{\mathcal{N}-1} p(k) \sum_{i=0}^k i \frac{k!}{i!(k-i)!} \left(\frac{x'}{x' + y'} \right)^i \\
&\quad \times \left(\frac{y'}{x' + y'} \right)^{k-i} \frac{i}{z} \\
&= \left(\frac{x'}{x' + y'} \right) + \left(\frac{\sigma^2 + z^2 - z}{z} \right) \left(\frac{x'}{x' + y'} \right)^2. \tag{8}
\end{aligned}$$

Similarly, for the defector component the evaluated expression is given by

$$\begin{aligned}
\lim_{\Delta t \rightarrow 0} \frac{1}{\Delta t} \sum_{j=0}^{\mathcal{N}} \sum_{i=0}^{\mathcal{N}-j} [jT_j^- P(i, j, t)] \Delta t &= \sum_{j=0}^{\mathcal{N}} jT_j^- P_j(j, t) \\
&= \left(\frac{y'}{x' + y'} \right) + \left(\frac{\sigma^2 + z^2 - z}{z} \right) \left(\frac{y'}{x' + y'} \right)^2. \tag{9}
\end{aligned}$$

- Next, we are interested to measure the possibility whether the particular individual population could be influenced by outside individuals or not, where this mathematical part deals with the analytical deriving procedure to capture the effect of the random drift phenomenon to the evolutionary dynamics. Here, we measure the random drift effect on the probability space Ω which is defined as $\Omega = \{(p = zp', q) : 0 \leq p \leq 1, 0 \leq q \leq 1\}$ where p' is the probability of attachment of a new individual at the per degree of a vertex and q is the probability of leaving of an individual at the maximum degree of a vertex; clearly in the sense of probability in the one dimensional space we get: $q \leq -q \equiv p$. However, one dimension is not our concern presently. Now, introducing a dummy small space length $2\Delta h$ and the fractional concentration variable $x = \left(\frac{1}{\mathcal{N}} \right) \lim_{\Delta h \rightarrow 0} \frac{x'}{(2\Delta h)^2}$, equating the conservation law and the concept of continuous probability law, intuitively it can be written as

$$\begin{aligned}
\lim_{\Delta t \rightarrow 0} \frac{1}{\Delta t} \sum_{i=0}^{\mathcal{N}} \sum_{j=0}^{\mathcal{N}-i} [iT_{i+1}^- P(i+1, j, t) - iT_i^- P(i, j, t)] \Delta t &\propto 2\Delta h \cdot \frac{\partial}{\partial p} x(p + \Delta h, q, t) \\
&\quad - 2\Delta h \cdot \frac{\partial}{\partial p} x(p - \Delta h, q, t) - 2\Delta h \cdot \frac{\partial}{\partial q} x(p, q + \Delta h, t) \\
&\quad + 2\Delta h \cdot \frac{\partial}{\partial q} x(p, q - \Delta h, t) = (2\Delta h)^2 \left(\frac{\partial^2 x}{\partial p^2} - \frac{\partial^2 x}{\partial q^2} \right) \\
&= (2\Delta h)^2 \nabla^2 x. \tag{10}
\end{aligned}$$

Similarly, with the fractional concentration variable $y = \left(\frac{1}{\mathcal{N}} \right) \lim_{\Delta h \rightarrow 0} \frac{y'}{(2\Delta h)^2}$, for the defector component the evaluated expression is given by

$$\begin{aligned}
\lim_{\Delta t \rightarrow 0} \frac{1}{\Delta t} \sum_{i=0}^{\mathcal{N}} \sum_{j=0}^{\mathcal{N}-i} [jT_{j+1}^- P(i, j+1, t) - iT_i^- P(i, j, t)] \Delta t &\propto 2\Delta h \cdot \frac{\partial}{\partial p} y(p + \Delta h, q, t) \\
&- 2\Delta h \cdot \frac{\partial}{\partial p} y(p - \Delta h, q, t) - 2\Delta h \cdot \frac{\partial}{\partial q} y(p, q + \Delta h, t) \\
&+ 2\Delta h \cdot \frac{\partial}{\partial q} y(p, q - \Delta h, t) = (2\Delta h)^2 \left(\frac{\partial^2 y}{\partial p^2} - \frac{\partial^2 y}{\partial q^2} \right) \\
&= (2\Delta h)^2 \bar{\nabla}^2 y.
\end{aligned} \tag{11}$$

Therefore, introducing the proportional constants σ_x, σ_y and scale factor $\alpha = \frac{1}{\mathcal{N}}$, the dynamical discrete equations turn out to be the continuous equations having the following forms:

$$\frac{\partial x}{\partial t} = a_3 \left(\frac{x}{x+y} \right)^3 + a_2 \left(\frac{x}{x+y} \right)^2 + a_1 \left(\frac{x}{x+y} \right) + \sigma_x \bar{\nabla}^2 x, \tag{12}$$

$$\frac{\partial y}{\partial t} = b_3 \left(\frac{y}{x+y} \right)^3 + b_2 \left(\frac{y}{x+y} \right)^2 + b_1 \left(\frac{y}{x+y} \right) + \sigma_y \bar{\nabla}^2 y, \tag{13}$$

where $a_3 = \left(\frac{\pi_{CC} - \pi_{CD}}{\Gamma_{max}} \right) \left(\frac{\sigma^2 + z^2 - z}{z} \right) \alpha$, $a_2 = \left(\frac{\sigma^2 + z^2 - z}{z} \right) \left(\frac{\pi_{CD}}{\Gamma_{max}} - 1 \right) \alpha + \left(\frac{\pi_{CC} - \pi_{CD}}{\Gamma_{max}} \right) \alpha$, $a_1 = \left(\frac{\pi_{CD}}{\Gamma_{max}} - 1 \right) \alpha$, $b_3 = \left(\frac{\pi_{DD} - \pi_{DC}}{\Gamma_{max}} \right) \left(\frac{\sigma^2 + z^2 - z}{z} \right) \alpha$, $b_2 = \left(\frac{\sigma^2 + z^2 - z}{z} \right) \left(\frac{\pi_{DC}}{\Gamma_{max}} - 1 \right) \alpha + \left(\frac{\pi_{DD} - \pi_{DC}}{\Gamma_{max}} \right) \alpha$, $b_1 = \left(\frac{\pi_{DC}}{\Gamma_{max}} - 1 \right) \alpha$, $\alpha t = t'$; and nabla-bar-square measures the net effect of random drift in respect of the probability space, Ω . As we consider the evolutionary dynamics on network in a finite population, the upper limit of concentration is to be confined by the explicit involvement of total allocable space \mathcal{N} in both of above equations; in the change of time scale this involvement totally depends on the specific values of other equation parameters and the trick enables us to measure the whole scenario of evolution in the same scale-up calibration under the constrains of $x \geq 0, y \geq 0$ and $x + y \leq 1$, and in the consideration of a periodic boundary condition in (p, q) -space. The Fig. 2 shows the three panel analytical outcome.

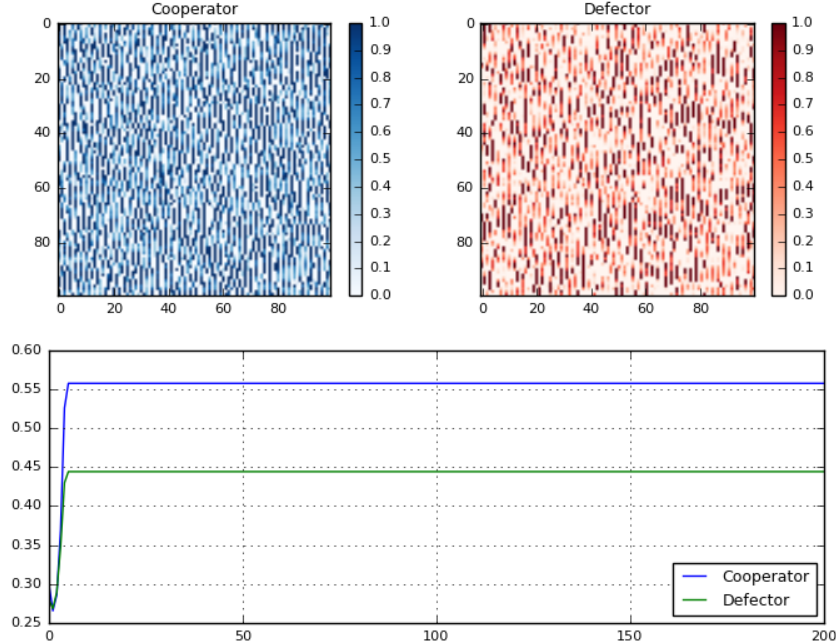


Figure 2: Upper panels: The final concentration distributions of cooperators and defectors over Ω field of 10,000 observation points; Lower panel: The analytical version outcomes up to 20,000 time steps at the point $(p, q) = (0.5, 0.4)$. The data corresponding to the base matrix of Fig. 4 are used.

2.2 The algorithm version of the evolutionary dynamics

Definitely, the first part of the update process, birth-death, is a slow process than the random drift. Without loss of generality, we assume that its completion time takes 15 time steps. In a neighbourhood area, in the presence of i -number of C individuals and j -number of D individuals, the focal C individual gives birth an offspring by Moran rule of: $\text{random}() < \frac{i \cdot \pi_{CC} + j \cdot \pi_{CD}}{z \cdot \Gamma_{max}}$, where the death of the focal individual occurs by the Moran rule of: $\text{random}() < \frac{i}{z}$; and similar to a focal D individual. Regarding each of the complement probabilities, an individual will not participate in evolution process and the system will remain unaltered. The derived algorithm version is a proper map of the continuous evolution version undoubtedly. Under the synchronous consideration, the newborn offspring is placed in empty vertex and if it is not possible, then the offspring takes any randomly chosen place of the neighbourhood. We obtain a scaling in $\mathcal{O}(z)$. Every individual goes through the evolution process at most once in each generation which has been defined by the 15 time steps. The time complexity of the whole birth-death computation is of the order $\mathcal{O}(\mathcal{N})$.

On the continuous probability space, in the limit of $\Delta h \rightarrow 0$, the increasing rate of an event of certainty about random drift with positive sign and the decreasing rate of an event of certainty about random drift with negative sign interpret the randomness at the point (p, q) , in the sense that the measurement assumes either positive value, negative value or zero. In the discrete algorithm case, at the point (p, q) mathematically the randomness of net effectiveness of drift on an individual where the possibility of drifted individual type is selected by the majority ratio of the individual type in the neighbourhood area including the focal individual itself is determined separately; an individual attachment rule is of: $\text{random}() < p \cdot \sigma_*$, an individual leaving rule is of: $\text{random}() < q \cdot \sigma_*$, and in the case of complementary probability the rules are unaffected in which the generated random number is outside of the range. The outside influence possibility on the evolution is measured by the random drift along with the local possibility of the birth-death. The both the inequalities are considered simultaneously at a particular point where the random drift constant σ_* controls the speed of the drift. Under the synchronous consideration, a newcomer individual is placed at a vacant vertex and if it is not

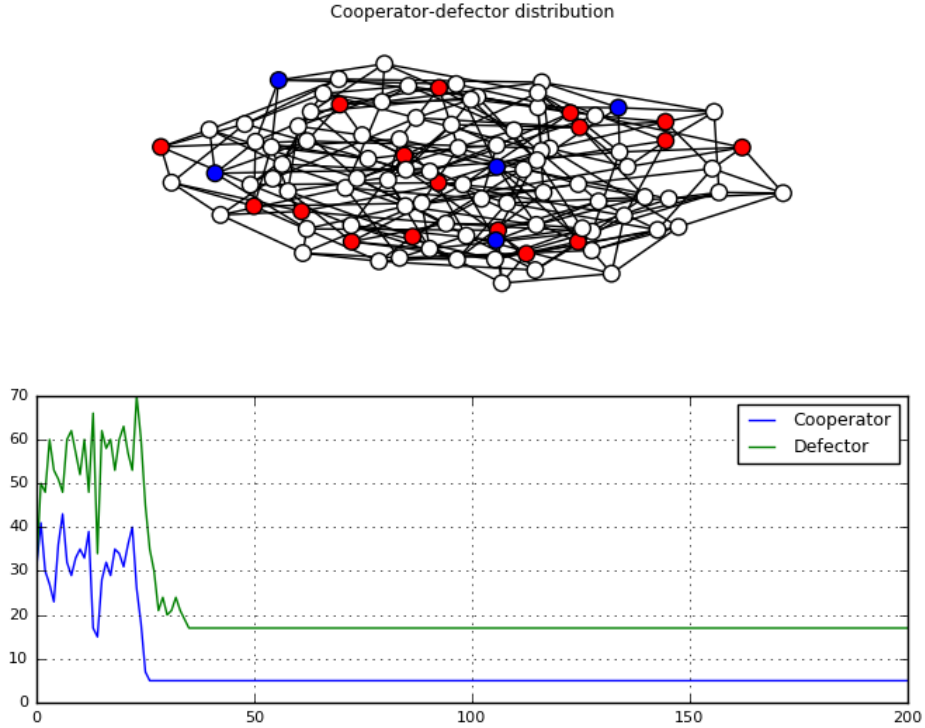


Figure 3: One of the algorithm version outcomes for $\mathcal{N} = 100$ up to 20,000 time steps. Without random drift, the base matrix concerning experimental outcome of the Fig. 4 is depicted here.

possible then the newcomer replaces the focal individual. We obtain a scaling in $\mathcal{O}(z)$. Every vertex site go through the random drift process at most once in each time step. Undoubtedly, here also, the both measurement methods – continuous and discrete – is two sides of the same coin. The time complexity of the random drift computation is of the order $\mathcal{O}(\mathcal{N})$.

We use Python library, NetworkX [23], for studying the algorithmic dynamics on networks [24]. The Fig. 3 shows the two panel algorithm outcome.

3 The significance of parameters

In order to define the term $\frac{0}{0}$ to be equal to 0 we introduce a bound K such that $0 \leq x + y < K$ and for such introduction we have $\frac{x}{x+y} = \frac{x}{K} (1 + \frac{x+y-K}{K})^{-1} \approx \frac{x}{K^2} (2K - x - y)$, and similarly for $\frac{y}{x+y}$.

The temporal dynamics possesses the trivial equilibrium $(0, 0)$ and one axial equilibrium at the position $(\tilde{x}, 0)$ for $a_1 + a_2 + a_3 = 0$ when $\Gamma_{max} = b - c$; however, the $(0, \tilde{y})$ is not an equilibrium point since at this position $b_1 + b_2 + b_3 = -(\frac{\sigma^2 + z^2 - z}{z} + 1)$.

In the linearised temporal dynamics the associated Jacobian matrix at the trivial equilibrium is of the form: $M_{(0,0)} = \begin{pmatrix} \frac{2a_1}{K} & 0 \\ 0 & \frac{2b_1}{K} \end{pmatrix}$. If both eigenvalues are negative, the trivial equilibrium is stable here. Introducing, $X = \begin{pmatrix} x \\ y \end{pmatrix}$, $\sigma = \begin{pmatrix} \sigma_x \\ \sigma_y \end{pmatrix}$ and considering $\nabla^2 X = -\lambda X$ with $\lambda > 0$, at the trivial equilibrium the characteristic matrix of the drift-augmented Jacobian matrix in term of the temporal eigenvalue κ , is of the form: $\kappa I - M_{(0,0)} + \lambda \sigma = \begin{pmatrix} \kappa - \frac{2a_1}{K} + \lambda \sigma_x & 0 \\ 0 & \kappa - \frac{2b_1}{K} + \lambda \sigma_y \end{pmatrix}$. That is the characteristic equation is given by: $\kappa^2 + d_1(\lambda)\kappa + d_2(\lambda) = 0$, where $d_1(\lambda) = (\sigma_x + \sigma_y)\lambda - (\frac{2a_1}{K} + \frac{2b_1}{K})$ and $d_2(\lambda) = \lambda^2 - (\frac{2a_1}{\sigma_x K} + \frac{2b_1}{\sigma_y K})\lambda + \frac{4a_1 b_1}{\sigma_x \sigma_y K^2}$. As both, d_1 and d_2 , is positive, the occurrence of Turing instability [25, 26] is not possible. However, numerical outcomes clearly make aware of us that on the (p, q) -space the most of the points shows the unstable dynamic character. Therefore, our assumption about the negative value of spatial eigenvalue, $-\lambda$, for each point is not correct – because we do not know the distribution nature of the spatial eigenvalues on the probability space – where the cooperator will act as activator under the consideration of $\frac{2a_1}{K} < \sigma_x$ while the defector will act as inhibitor under the consideration of $|\frac{2b_1}{K}| > \sigma_y$. Here, the positive spatial eigenvalue indicates that the individuals enter into the considering area.

In the linearised temporal dynamics the associated Jacobian matrix at the axial equilibrium is of the form: $M_{(\tilde{x},0)} = \begin{pmatrix} 0 & -\frac{1}{\tilde{x}}(2a_3 + a_2) \\ 0 & \frac{b_1}{\tilde{x}} \end{pmatrix}$. As one of the eigenvalues is zero and the other is negative, thus the axial equilibrium is non-hyperbolic where the Hartman-Grobman Theorem is not applicable.

It is naturally expected that before both types of individuals go extinct or in their internal position they can form a non-hyperbolic equilibrium state which defines the non-trivial equilibrium, but to find out an internal equilibrium in the system is not possible in general by the differential equation rule as conservation principle is not directly used here; however we can obtain internal equilibrium by imposing a constrain through the stepwise procedure. If $K \approx 0$, then we can determine a non-hyperbolic equilibrium point (\tilde{x}, \tilde{y}) such that $\tilde{x} + \tilde{y} = 2K$, where the activation role and inhabitation role is settled by the pair $(\frac{a_1 \tilde{y}}{4K^2}, \frac{b_1 \tilde{x}}{4K^2})$ on the centre manifold. We know that the dynamics around non-hyperbolic points is not robust. Adding non-linearities terms and/or changing parameters may lead to strong unpredictability.

4 Method outline and outcome

Unlike the previous studies [27, 28, 29], the two distinct evolutionary mechanisms have been described on the random regular graph of degree z . In each of the initial stages at the attempt of equal distribution, it is tried to randomly assign the cooperators, defectors and vacant places over the vertices of the graph so that none of the types get an additional advantage in their evolutionary process. The synchronous model update combines the two steps: one is the birth-death update where the pair do not fully depend on each other, and second one is the random drift step where the preferential type chooses on the concept: the like-minded individuals would always attract to each other and the act is operated by the majority selection rule. Without loss of generality, we take 15 time steps as one generation in which either the birth or the death occurs at most once. However, according to normal law the birth-death step gets more preference

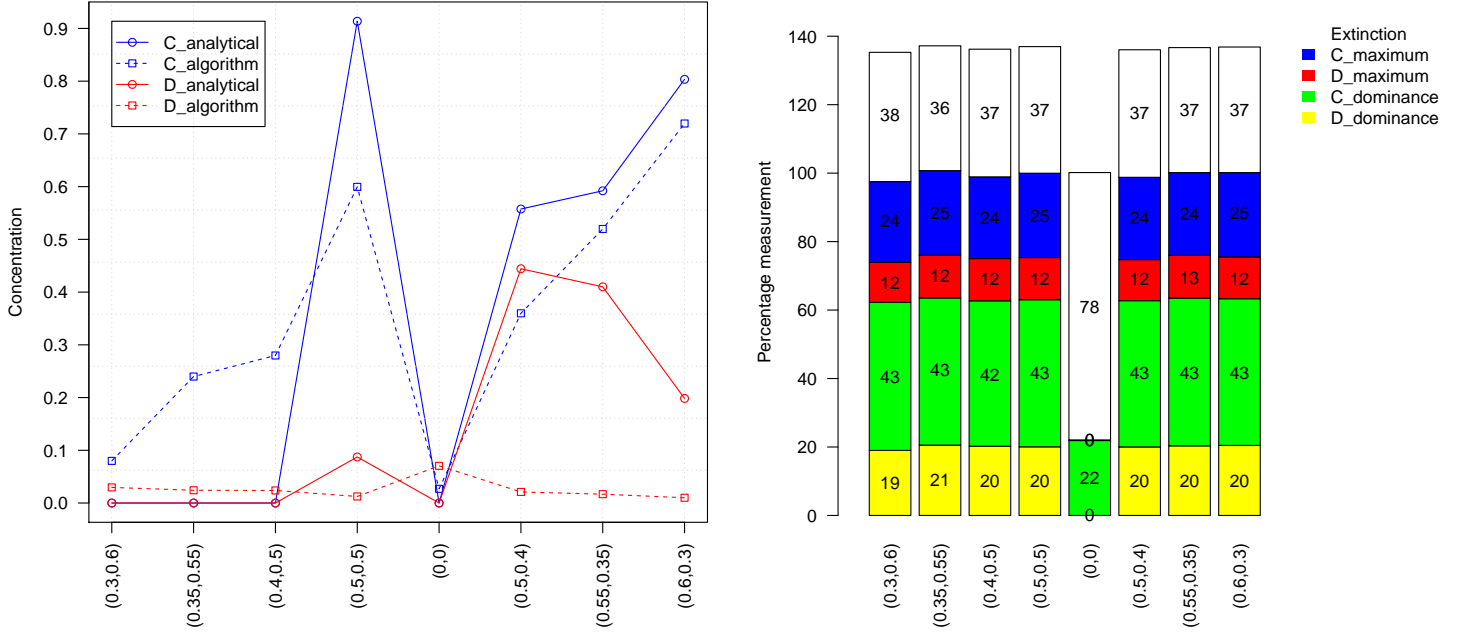


Figure 4: Left panel: The qualitative comparison between the evolutionary outcomes of the analytical procedure and the algorithm method; Right panel: The percentage measurement based on the 10,000 observations related to evolutionary outcome at each grid site of the analytical procedure. The outcomes after 20,000 time steps with a generation interval of 0.02 time scale are examined in consideration of maximum fitness, 0.77, and of fitness payoffs: $\pi_{CC} = 1.5$, $\pi_{CD} = -0.3$, $\pi_{DC} = 1.8$, $\pi_{DD} = 0$. The number of allocable vertices and the degree of the graph respectively are 1000 and 50 where the random drift coefficient in the analytical procedure and the algorithm method respectively is 10^{-5} and 0.3×10^{-1} .

than the random drift evolutionary step. The algorithm experiment data are collected by averaging over the outcome values for running the program up to 20,000 time steps in the 25 different graph structure realisations.

We select the same initial averaging concentration value in the analytical procedure at the particular point of evolutionary observation, in the Fig. 2 the point is (0.5, 0.4) where initial concentrations of other observation points assign by the uniform distribution law, applied in the range (0, 0.3). The analytical procedure acts as a correcter tool and run it several times to correct our algorithmic prediction. Both the periodical condition and the bounded condition: $x + y \leq 1$, take into the consideration on the physical space of 100×100 locations; each location as a point linearly maps to Ω space.

The outcomes of both evolutionary mechanisms related to the analytics and the algorithm, ensure the ubiquitous character of cooperation in the presence of the random drift. The (p, q) data-range represents the comparison outcomes (the Left panel of Fig. 4). The both independent quantities p and q have been considered as random variables in respect of time scale, while in another turn where time scale is insignificant those act as non random parameter variables. For different aspects, an arbitrary variable can have such dual character simultaneously. In the model development, we use this intuitive sense.

In the Right panel of Fig. 4 the five dependent observables in the scale of 0 (or extinction) to 1 (or maximum – the state of all C or all D) are introduced. The observables are self-explanatory and have been counted on 10000 observation points. The experiment is carried out over three game classes, namely, Dominance game, Coexistence game and Coordination game with either $\mathcal{N} = 100$ or $\mathcal{N} = 1000$, where we uniformly set initial conditions so that either of types do not get an initial advantage in every possible position, but the uniform distribution of the random initial conditions has its own limitation [30]. According to expectation in mixed population where defectors have higher fitness than cooperators natural selection favors defectors. However, in the absence of random drift we even observe the phenomenon of the defector extinction. This observation has a simple interpretation. In the intratype competition defector fitness payoff is either zero or very minimum, and as a consequence, in the presence of a low number of

cooperators survival capacity of defectors markedly reduces and ultimately they become extinct in the most of the possible situations.

5 Conclusion

The visualised experimental data along with data in the Supplementary material, measure the efficiency of the random drift at sustaining cooperation. In fact, the unbiased attachment rule lays down the equal probable situation for attachment of two types. However, attachment of relatively more defectors than the cooperators leads to extinction, while the attachment of cooperators increases the survival capacity of individuals, irrespective of their behaviour. As extinction environment does not have any effect on the plausible survey result of individual promoting, the evolution track always revealed the fact of cooperation emerging and enhance in front of our eyes. This is why cooperative behaviour is very natural to observe in various forms of our life system. The explanation does not violate our belief that under the neutral role play, natural environment always tries to retain the environment of coexistence traits [31, 32, 33] – the state of biodiversity.

Of particular note is under the ranges of the model parameters the value of $b_1 + b_2 + b_3$ which is never equal to zero; consequently, we can not consider the point $(0, \tilde{y})$ as an equilibrium point and it provides us the reason for the arising question about the chance of survival of defectors without cooperator while $a_1 + a_2 + a_3$ equal to zero can be evaluated, means that $(\tilde{x}, 0)$ can be an equilibrium point in the evolutionary process. Also one of the explanations of pattern formation through Turing instability [34] is completely ruled out in this mathematical formalism since the priori assumption $\nabla^2 \left(\frac{x}{y} \right) = -\lambda \left(\frac{x}{y} \right)$ with spatial eigenvalue, λ , greater than zero is not acceptable for every point on Ω field. Even though if we accept this in some compromise sense probability to occur pattern formation will be almost zero.

Here, in the many circumstances, as fitnesses of individuals depend on the frequencies of cooperators and defectors, the Fisher's fundamental theorem of natural selection which states that average fitness is increased or remains the same under constant selection does not hold. Concerning the same topic it is worth mentioning that the Hardy-Weinberg law [35] approved by this mathematical formalism is to be interpreted by, $\dot{x} = \dot{y} = 0$, at the set payoff values equal to a constant value.

A comparison has been made between the algorithm method and the analytical procedure due to the intention to demonstrate the natural cooperation characterised by a principle rather than a specific rule of an environmental scenario. For conducting the experiments we consider all possible interrelations among fitness values of two different types of individuals where one can realise that algorithm version is good for a better prediction to point out the initial direction and to find out the final outcome of evolutionary fate while the analytical procedure being good tracer of the intermediate evolutionary path. The evolutionary path which governs by many of the unpredictable characters of nature to be explained by preassigned strict rules (or randomly ever-changing set of interactors) over a long time is some extend unrealistic while the analytic one entailed by the average sense can produce closed realistic evolutionary results. Because of this intuitive belief, we use the algorithm version as a predictor tracer and the analytical version as a corrector tracer of an evolutionary path. We anticipate our purely mathematical treatment to be a better choice than the agent-based method [36] to simulate the complexity of heterogeneous populations. The simple design structure, in particular the nabla-bar-square will have great potential for examining a topological dynamical system in the higher dimension, and to gain the knowledge we have to walk the extra mile.

In this article we show that the evolution about genetic variation, combining the effects of the social evolution of the birth-death on network structure and of the random drift, gives the final verdict on the selection of the individual type. The social evolution, defined also by average birth-death effect in term of the pure replicator equation, depends only on constant fitness values of individuals and reasonably its outcomes are nothing but the normal display of the linear impact of the payoff-to-fitness mapping and consequently it might be failing to attain a generality. The one of the factors considering for cooperation enhancement is the effect of a social network structure. However, it would be expected for unbiased distribution of individuals, both types of individual would get equal benefit from the social structure effect. Therefore, one simple conclusion is that over a long evolutionary process the feature of the intratype interaction acts the key role in cooperation enhancement and defection hindrance where the driving force of lending a helping hand of themselves provides the instrumental clues to their future evolutionary fate.

6 Supplementary material

Additional materials as a separate file under the heading of Supplementary Material accompanies the paper in Latex Source Files.

7 Research data

The main model code is available in GitHub with identifier <https://github.com/bijan0317/cdevolution.git>

References

- [1] Bahram Houchmandzadeh. Fluctuation driven fixation of cooperative behavior. *Biosystems*, 127:60 – 66, 2015.
- [2] Weini Huang, Christoph Hauert, and Arne Traulsen. Stochastic game dynamics under demographic fluctuations. *Proceedings of the National Academy of Sciences*, 112(29):9064 – 9069, 2015.
- [3] Alex McAvoy, Nicolas Fraiman, Christoph Hauert, John Wakeley, and Martin A Nowak. Public goods games in populations with fluctuating size. *Theoretical population biology*, 121:72 – 84, 2018.
- [4] James Mallet. The struggle for existence: how the notion of carrying capacity, k , obscures the links between demography, darwinian evolution, and speciation. *Evolutionary Ecology Research*, 14:627 – 665, 2012.
- [5] Christoph Hauert and Michael Doebeli. Spatial structure often inhibits the evolution of cooperation in the snow-drift game. *Nature*, 428(6983):643 – 646, 2004.
- [6] Kaj-Kolja Kleineberg. Metric clusters in evolutionary games on scale-free networks. *Nature communications*, 8(1):1888, 2017.
- [7] Arne Traulsen, Jens Christian Claussen, and Christoph Hauert. Coevolutionary dynamics: from finite to infinite populations. *Physical review letters*, 95(23):238701, 2005.
- [8] Walter F Bodmer. Differential fertility in population genetics models. *Genetics*, 51(3):411 – 424, 1965.
- [9] JF Kidwell, MT Clegg, FM Stewart, and T Prout. Regions of stable equilibria for models of differential selection in the two sexes under random mating. *Genetics*, 85(1):171 – 183, 1977.
- [10] Bijan Sarkar. Random and non-random mating populations: Evolutionary dynamics in meiotic drive. *Mathematical biosciences*, 271:29 – 41, 2016.
- [11] Nicolas Champagnat, Régis Ferrière, and Sylvie Méléard. Unifying evolutionary dynamics: from individual stochastic processes to macroscopic models. *Theoretical population biology*, 69(3):297 – 321, 2006.
- [12] Burton Simon. A stochastic model of evolutionary dynamics with deterministic large-population asymptotics. *Journal of Theoretical Biology*, 254(4):719 – 730, 2008.
- [13] Michael Doebeli, Yaroslav Ispolatov, and Burt Simon. Point of view: Towards a mechanistic foundation of evolutionary theory. *Elife*, 6:e23804, 2017.
- [14] Hisashi Ohtsuki, Christoph Hauert, Erez Lieberman, and Martin A Nowak. A simple rule for the evolution of cooperation on graphs and social networks. *Nature*, 441(7092):502 – 505, 2006.
- [15] Martin A Nowak. Five rules for the evolution of cooperation. *science*, 314(5805):1560 – 1563, 2006.
- [16] David G Rand and Martin A Nowak. Human cooperation. *Trends in cognitive sciences*, 17(8):413 – 425, 2013.
- [17] Francisco C Santos, Marta D Santos, and Jorge M Pacheco. Social diversity promotes the emergence of cooperation in public goods games. *Nature*, 454(7201):213 – 216, 2008.
- [18] Minus Van Baalen and David A Rand. The unit of selection in viscous populations and the evolution of altruism. *Journal of theoretical biology*, 193(4):631 – 648, 1998.
- [19] Mark Broom and Jan Rychtár. *Game-theoretical models in biology*. CRC Press, 2013.
- [20] Laura Hindersin, Bin Wu, Arne Traulsen, and Julian García. Computation and simulation of evolutionary game dynamics in finite populations. *Scientific reports*, 9(1):6946, 2019.
- [21] Crispin W Gardiner. *Handbook of stochastic methods*, volume 3. springer Berlin, 1985.
- [22] James F Crow and Motoo Kimura. *An introduction to population genetics theory*. Harper & Row, New York, 1970.
- [23] Aric Hagberg, Pieter Swart, and Daniel S Chult. Exploring network structure, dynamics, and function using networkx. Technical report, Los Alamos National Lab.(LANL), Los Alamos, NM (United States), 2008.
- [24] Mark Newman. *Networks*. Oxford university press, 2018.
- [25] Nicholas F Britton. *Essential mathematical biology*. Springer Science & Business Media, 2012.

-
- [26] Alexey M Nesterenko, Maxim B Kuznetsov, Daria D Korotkova, and Andrey G Zaraisky. Morphogene adsorption as a Turing instability regulator: Theoretical analysis and possible applications in multicellular embryonic systems. *PLoS one*, 12(2):e0171212, 2017.
- [27] Erez Lieberman, Christoph Hauert, and Martin A Nowak. Evolutionary dynamics on graphs. *Nature*, 433(7023):312 – 316, 2005.
- [28] Joshua Zukewich, Venu Kurella, Michael Doebeli, and Christoph Hauert. Consolidating birth-death and death-birth processes in structured populations. *PLoS One*, 8(1):e54639, 2013.
- [29] Benjamin Allen, Gabor Lippner, Yu-Ting Chen, Babak Fotouhi, Naghmeh Momeni, Shing-Tung Yau, and Martin A Nowak. Evolutionary dynamics on any population structure. *Nature*, 544(7649):227 – 230, 2017.
- [30] Matjaž Perc, Jillian J Jordan, David G Rand, Zhen Wang, Stefano Boccaletti, and Attila Szolnoki. Statistical physics of human cooperation. *Physics Reports*, 687:1 – 51, 2017.
- [31] Tobias Reichenbach, Mauro Mobilia, and Erwin Frey. Mobility promotes and jeopardizes biodiversity in rock-paper-scissors games. *Nature*, 448(7157):1046 – 1049, 2007.
- [32] Wes Maciejewski, Feng Fu, and Christoph Hauert. Evolutionary game dynamics in populations with heterogeneous structures. *PLoS computational biology*, 10(4):e1003567, 2014.
- [33] Bijan Sarkar. Moran-evolution of cooperation: From well-mixed to heterogeneous complex networks. *Physica A: Statistical Mechanics and its Applications*, 497:319 – 334, 2018.
- [34] Hiroya Nakao and Alexander S Mikhailov. Turing patterns in network-organized activator-inhibitor systems. *Nature Physics*, 6(7):544, 2010.
- [35] Warren J Ewens. *Mathematical population genetics 1: theoretical introduction*, volume 27. Springer Science & Business Media, 2012.
- [36] Christoph Adami, Jory Schossau, and Arend Hintze. Evolutionary game theory using agent-based methods. *Physics of life reviews*, 19:1 – 26, 2016.